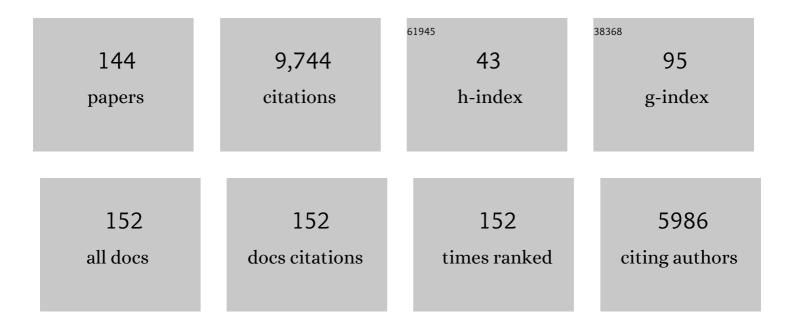
## Moataz Attallah

List of Publications by Year in descending order

Source: https://exaly.com/author-pdf/5781689/publications.pdf Version: 2024-02-01



#	Article	IF	CITATIONS
1	Synchrotron Characterisation of Ultra-Fine Grain TiB2/Al-Cu Composite Fabricated by Laser Powder Bed Fusion. Acta Metallurgica Sinica (English Letters), 2022, 35, 78-92.	1.5	8
2	Experimental and numerical investigations on the process quality and microstructure during induction heating assisted incremental forming of Ti-6Al-4V sheet. Journal of Materials Processing Technology, 2022, 299, 117323.	3.1	22
3	Development of Ni-base metal matrix composites by powder metallurgy hot isostatic pressing for space applications. Advanced Powder Technology, 2022, 33, 103411.	2.0	21
4	Effect of Stoichiometry on Shape Memory Properties of Ti-Ni-Hf-Cu-Nb Shape Memory Alloys Manufactured by Suspended Droplet Alloying. Solids, 2022, 3, 1-21.	1.1	0
5	Microstructure, tensile properties of SLMed TNT5Zr-0.2O alloys without/with keyholes produced by different Post-processing treatments. Materials Letters, 2022, 309, 131448.	1.3	0
6	Microstructural characterisation and high-temperature oxidation of laser powder bed fusion processed Inconel 625. Materials Letters, 2022, 311, 131582.	1.3	7
7	In situ neutron diffraction unravels deformation mechanisms of a strong and ductile FeCrNi medium entropy alloy. Journal of Materials Science and Technology, 2022, 116, 103-120.	5.6	16
8	Hybrid Electron Beam Powder Bed Fusion Additive Manufacturing of Ti–6Al–4V: Processing, Microstructure, and Mechanical Properties. Metallurgical and Materials Transactions A: Physical Metallurgy and Materials Science, 2022, 53, 927-941.	1.1	2
9	A 3-D Printed 300 GHz Waveguide Cavity Filter by Micro Laser Sintering. IEEE Transactions on Terahertz Science and Technology, 2022, 12, 274-281.	2.0	12
10	Deformation of AlSi10Mg parts manufactured by Laser Powder Bed Fusion: In-situ measurements incorporating X-ray micro computed tomography and a micro testing stage. Procedia Structural Integrity, 2022, 35, 168-172.	0.3	1
11	Enabling high efficiency magnetic refrigeration using laser powder bed fusion of porous LaCe(Fe,Mn,Si)13 structures. Additive Manufacturing, 2022, 51, 102620.	1.7	0
12	The influence of advanced hot isostatic pressing on phase transformations, mechanical properties of Ti-34Nb-13Ta-5Zr-0.2O alloy manufactured by In-situ alloying via selective laser melting. Journal of Alloys and Compounds, 2022, 903, 163974.	2.8	3
13	Powder HIP of pure Nb and C-103 alloy: The influence of powder characteristics on mechanical properties. International Journal of Refractory Metals and Hard Materials, 2022, 104, 105803.	1.7	7
14	Effect of Oxygen Diffusion During the Post-Processing of Ti6Al4V Lattice Structures Fabricated by the Selective Laser Melting Process. Journal of Engineering Materials and Technology, Transactions of the ASME, 2022, 144, .	0.8	0
15	A Convolutional Neural Network (CNN) classification to identify the presence of pores in powder bed fusion images. International Journal of Advanced Manufacturing Technology, 2022, 120, 5133-5150.	1.5	15
16	Comparison of LPBF processing of AlSi40 alloy using blended and pre-alloyed powder. Additive Manufacturing Letters, 2022, 2, 100038.	0.9	4
17	A Narrowband 3-D Printed Invar Spherical Dual-Mode Filter With High Thermal Stability for OMUXs. IEEE Transactions on Microwave Theory and Techniques, 2022, 70, 2165-2173.	2.9	8
18	Development, characterisation, and modelling of processability of nitinol stents using laser powder bed fusion. Journal of Alloys and Compounds, 2022, 909, 164681.	2.8	24

#	Article	IF	CITATIONS
19	In-situ alloyed CoCrFeMnNi high entropy alloy: Microstructural development in laser powder bed fusion. Journal of Materials Science and Technology, 2022, 123, 123-135.	5.6	6
20	Temperature-dependent enthalpy and entropy stabilization of solid solution phases in non-equiatomic CoCrFeNiTi high entropy alloys: computational phase diagrams and thermodynamics. Modelling and Simulation in Materials Science and Engineering, 2022, 30, 045013.	0.8	1
21	Microstructural Evolution, Mechanical Properties, and Preosteoblast Cell Response of a Post-Processing-Treated TNT5Zr β Ti Alloy Manufactured via Selective Laser Melting. ACS Biomaterials Science and Engineering, 2022, 8, 2336-2348.	2.6	6
22	Thermal Stability Analysis of 3D Printed Resonators Using Novel Materials. , 2022, , .		3
23	Neural Network Modeling of NiTiHf Shape Memory Alloy Transformation Temperatures. Journal of Materials Engineering and Performance, 2022, 31, 10258-10270.	1.2	7
24	Revealing the microstructural evolution of electron beam powder bed fusion and hot isostatic pressing Ti-6Al-4V in-situ shelling samples using X-ray computed tomography. Additive Manufacturing, 2022, 57, 102962.	1.7	5
25	A high strength and low modulus metastable β Ti-12Mo-6Zr-2Fe alloy fabricated by laser powder bed fusion in-situ alloying. Additive Manufacturing, 2021, 37, 101708.	1.7	5
26	Machining and heat treatment as post-processing strategies for Ni-superalloys structures fabricated using direct energy deposition. Journal of Manufacturing Processes, 2021, 61, 236-244.	2.8	47
27	Influence of the laser source pulsing frequency on the direct laser deposited Inconel 718 thin walls. Journal of Alloys and Compounds, 2021, 856, 158095.	2.8	18
28	Microstructural and Mechanical Characterization of Thin-Walled Tube Manufactured with Selective Laser Melting for Stent Application. Journal of Materials Engineering and Performance, 2021, 30, 696-710.	1.2	24
29	New materials development. , 2021, , 529-562.		1
30	The role of powder atomisation route on the microstructure and mechanical properties of hot isostatically pressed Inconel 625. Materials Science & Engineering A: Structural Materials: Properties, Microstructure and Processing, 2021, 808, 140950.	2.6	13
31	Laser Powder Bed Fusion of Ti-6Al-2Sn-4Zr-6Mo Alloy and Properties Prediction Using Deep Learning Approaches. Materials, 2021, 14, 2056.	1.3	12
32	The effect of the heat treatments on the tool wear of hybrid Additive Manufacturing of IN718. Wear, 2021, 470-471, 203617.	1.5	20
33	Evolution of internal pores within AlSi10Mg manufactured by laser powder bed fusion under tension: As-built and heat treated conditions. Materials and Design, 2021, 204, 109645.	3.3	25
34	Monolithic 3D printed waveguide filters with wide spuriousâ€free stopbands using dimpled spherical resonators. IET Microwaves, Antennas and Propagation, 2021, 15, 1657-1670.	0.7	6
35	Additive manufacturing of bio-inspired multi-scale hierarchically strengthened lattice structures. International Journal of Machine Tools and Manufacture, 2021, 167, 103764.	6.2	74
36	Controlling microstructural and mechanical properties of direct laser deposited Inconel 718 via laser power. Journal of Alloys and Compounds, 2021, 872, 159588.	2.8	25

#	Article	IF	CITATIONS
37	In situ alloying based laser powder bed fusion processing of β Ti–Mo alloy to fabricate functionally graded composites. Composites Part B: Engineering, 2021, 222, 109059.	5.9	21
38	On the constitutive relationship between solidification cells and the fatigue behaviour of IN718 fabricated by laser powder bed fusion. Additive Manufacturing, 2021, 47, 102347.	1.7	3
39	Microstructure-magnetic shielding development in additively manufactured Ni-Fe-Mo soft magnet alloy in the as fabricated and post-processed conditions. Journal of Alloys and Compounds, 2021, 884, 161112.	2.8	9
40	Direct laser deposition of crack-free CM247LC thin walls: Mechanical properties and microstructural effects of heat treatment. Materials and Design, 2021, 211, 110123.	3.3	18
41	SLM Printed Waveguide Dual-Mode Filters With Reduced Sensitivity to Fabrication Imperfections. IEEE Microwave and Wireless Components Letters, 2021, 31, 1195-1198.	2.0	16
42	A Melt Pool Temperature Model in Laser Powder Bed Fabricated CM247LC Ni Superalloy to Rationalize Crack Formation and Microstructural Inhomogeneities. Metallurgical and Materials Transactions A: Physical Metallurgy and Materials Science, 2021, 52, 5221-5234.	1.1	6
43	The influence of zirconium content on the microstructure, mechanical properties, and biocompatibility of in-situ alloying Ti-Nb-Ta based β alloys processed by selective laser melting. Materials Science and Engineering C, 2021, 131, 112486.	3.8	16
44	Laser powder bed fusion of a Zr-alloy: Tensile properties and biocompatibility. Materials Letters, 2020, 259, 126897.	1.3	34
45	The Effect of Powder Characteristics on Build Quality of High-Purity Tungsten Produced via Laser Powder Bed Fusion (LPBF). Metallurgical and Materials Transactions A: Physical Metallurgy and Materials Science, 2020, 51, 1367-1378.	1.1	21
46	Fabricating CoCrFeMnNi high entropy alloy via selective laser melting in-situ alloying. Journal of Materials Science and Technology, 2020, 43, 40-43.	5.6	96
47	Compressive behavior of stretched and composite microlattice metamaterial for energy absorption applications. Composites Part B: Engineering, 2020, 184, 107715.	5.9	51
48	Deformation mechanisms of FeCoCrNiMo0.2 high entropy alloy at 77 and 15ÂK. Scripta Materialia, 2020, 178, 166-170.	2.6	41
49	Additive manufacturing of a topology-optimised multi-tube energy storage device: Experimental tests and numerical analysis. Applied Thermal Engineering, 2020, 180, 115878.	3.0	35
50	In-situ alloyed, oxide-dispersion-strengthened CoCrFeMnNi high entropy alloy fabricated via laser powder bed fusion. Materials and Design, 2020, 194, 108966.	3.3	69
51	Novel Hybrid Manufacturing Process of CM247LC and Multi-Material Blisks. Micromachines, 2020, 11, 492.	1.4	10
52	Finite Element Modeling of Machining Nickel Superalloy Produced By Direct Energy Deposition Process. Procedia Manufacturing, 2020, 47, 525-529.	1.9	7
53	Post Processing of 3D Printed Metal Scaffolds: a Preliminary Study of Antimicrobial Efficiency. Procedia Manufacturing, 2020, 47, 1106-1112.	1.9	20
54	Selective Laser Melting of Ti-6Al-4V: The Impact of Post-processing on the Tensile, Fatigue and Biological Properties for Medical Implant Applications. Materials, 2020, 13, 2813.	1.3	69

#	Article	IF	CITATIONS
55	Microstructural control during laser powder fusion to create graded microstructure Ni-superalloy components. Additive Manufacturing, 2020, 36, 101432.	1.7	16
56	Assessment of trapped powder removal and inspection strategies for powder bed fusion techniques. International Journal of Advanced Manufacturing Technology, 2020, 106, 4521-4532.	1.5	47
57	Classifying shape of internal pores within AlSi10Mg alloy manufactured by laser powder bed fusion using 3D X-ray micro computed tomography: Influence of processing parameters and heat treatment. Materials Characterization, 2020, 163, 110225.	1.9	45
58	Magnetic shielding promotion via the control of magnetic anisotropy and thermal Post processing in laser powder bed fusion processed NiFeMo-based soft magnet. Additive Manufacturing, 2020, 32, 101079.	1.7	9
59	Metal 3D Printed D-Band Waveguide to Surface Wave Transition. , 2020, , .		2
60	Monolithic 3Dâ€printed slotted hemisphere resonator bandpass filter with extended spuriousâ€free stopband. Electronics Letters, 2019, 55, 331-333.	0.5	8
61	Fracture of three-dimensional lattices manufactured by selective laser melting. International Journal of Solids and Structures, 2019, 180-181, 147-159.	1.3	28
62	Microstructural Development and Mechanical Properties of Friction Stir Welded Ferritic Stainless Steel AISI 409. Journal of Materials Engineering and Performance, 2019, 28, 6391-6406.	1.2	25
63	In-vitro Study of Effect of the Design of the Stent on the Arterial Waveforms. Procedia Structural Integrity, 2019, 15, 33-40.	0.3	2
64	Shaping and Slotting High-Q Spherical Resonators for Suppression of Higher Order Modes. , 2019, , .		10
65	3-D Printed Slotted Spherical Resonator Bandpass Filters With Spurious Suppression. IEEE Access, 2019, 7, 128026-128034.	2.6	29
66	The analogies between human development and additive manufacture: Expanding the definition of design. Cogent Engineering, 2019, 6, .	1.1	5
67	Influence of processing parameters on internal porosity and types of defects formed in Ti6Al4V lattice structure fabricated by selective laser melting. Materials Science & Engineering A: Structural Materials: Properties, Microstructure and Processing, 2019, 767, 138387.	2.6	58
68	Influence of powder characteristics on the microstructure and mechanical properties of HIPped CM247LC Ni superalloy. Materials and Design, 2019, 174, 107796.	3.3	35
69	In-situ alloying of AlSi10Mg+Si using Selective Laser Melting to control the coefficient of thermal expansion. Journal of Alloys and Compounds, 2019, 795, 8-18.	2.8	35
70	Cracking during thermal post-processing of laser powder bed fabricated CM247LC Ni-superalloy. Materials and Design, 2019, 174, 107793.	3.3	80
71	Effect of powder characteristics and oxygen content on modifications to the microstructural topology during hot isostatic pressing of an austenitic steel. Acta Materialia, 2019, 172, 6-17.	3.8	39
72	Laser Powder Bed Fusion of Ti-rich TiNi lattice structures: Process optimisation, geometrical integrity, and phase transformations. International Journal of Machine Tools and Manufacture, 2019, 141, 19-29.	6.2	93

#	Article	IF	CITATIONS
73	The design of additively manufactured lattices to increase the functionality of medical implants. Materials Science and Engineering C, 2019, 94, 901-908.	3.8	89
74	Design of a Metal 3-D Printed Corrugated Antenna. , 2019, , .		1
75	Phase Diagram and Mechanical Properties of a CoCrFeNi1??Ti? High Entropy Alloy Fabricated by Mechanical Alloying. , 2019, , .		0
76	Laser powder bed fusion at sub-atmospheric pressures. International Journal of Machine Tools and Manufacture, 2018, 130-131, 65-72.	6.2	47
77	Tailoring selective laser melting process for titanium drug-delivering implants with releasing micro-channels. Additive Manufacturing, 2018, 20, 144-155.	1.7	45
78	Influence of the kissing bond on the mechanical properties and fracture behaviour of AA5083-H112 friction stir welds. Materials Science & Engineering A: Structural Materials: Properties, Microstructure and Processing, 2018, 719, 12-20.	2.6	44
79	The barriers to the progression of additive manufacture: Perspectives from UK industry. International Journal of Production Economics, 2018, 198, 104-118.	5.1	157
80	Additive manufacturing of magnetic shielding and ultra-high vacuum flange for cold atom sensors. Scientific Reports, 2018, 8, 2023.	1.6	24
81	Porosity control in 316L stainless steel using cold and hot isostatic pressing. Materials and Design, 2018, 138, 21-29.	3.3	47
82	Fluid and particle dynamics in laser powder bed fusion. Acta Materialia, 2018, 142, 107-120.	3.8	367
83	Netshape centrifugal gel-casting of high-temperature sialon ceramics. Ceramics International, 2018, 44, 3440-3447.	2.3	6
84	Linking microstructure and processing defects to mechanical properties of selectively laser melted AlSi10Mg alloy. Theoretical and Applied Fracture Mechanics, 2018, 98, 123-133.	2.1	92
85	Effect of Microstructure on the Morphology of Atmospheric Corrosion Pits in Type 304L Stainless Steel. Corrosion, 2018, 74, 1373-1384.	0.5	14
86	Controlling the grain orientation during laser powder bed fusion to tailor the magnetic characteristics in a Ni-Fe based soft magnet. Acta Materialia, 2018, 158, 230-238.	3.8	49
87	Suspended dropletÂalloying: A new method for combinatorial alloy synthesis; nitinol-based alloys as an example. Journal of Alloys and Compounds, 2018, 768, 392-398.	2.8	5
88	Laser powder bed fusion in high-pressure atmospheres. International Journal of Advanced Manufacturing Technology, 2018, 99, 543-555.	1.5	56
89	The Influence of Processing Parameters on Strut Diameter and Internal Porosity in Ti6Al4V Cellular Structure. , 2018, , .		0
90	Composite Powder Consolidation Using Selective Laser Melting: Input Energy/Porosity Morphology/Balling Effect Relation. Minerals, Metals and Materials Series, 2017, , 169-180.	0.3	4

Moataz Attallah

#	Article	IF	CITATIONS
91	Microstructure and yield strength of SLM-fabricated CM247LC Ni-Superalloy. Acta Materialia, 2017, 128, 87-95.	3.8	242
92	Evolution of grain boundary network topology in 316L austenitic stainless steel during powder hot isostatic pressing. Acta Materialia, 2017, 133, 269-281.	3.8	50
93	Development and testing of an additively manufactured monolithic catalyst bed for HTP thruster applications. Applied Catalysis A: General, 2017, 542, 125-135.	2.2	64
94	Net-shape manufacturing using hybrid selective laser melting/hot isostatic pressing. Rapid Prototyping Journal, 2017, 23, 720-726.	1.6	34
95	Surface Finish has a Critical Influence on Biofilm Formation and Mammalian Cell Attachment to Additively Manufactured Prosthetics. ACS Biomaterials Science and Engineering, 2017, 3, 1616-1626.	2.6	40
96	Spatial variation of microtexture in linear friction welded Ti-6Al-4V. Materials Characterization, 2017, 127, 342-347.	1.9	15
97	Mesoscale modelling of selective laser melting: Thermal fluid dynamics and microstructural evolution. Computational Materials Science, 2017, 126, 479-490.	1.4	227
98	Additive manufacturing of Ni-based superalloys: The outstanding issues. MRS Bulletin, 2016, 41, 758-764.	1.7	194
99	Microstructural control in a Ti-based alloy by changing laser processing mode and power during direct laser deposition. Materials Letters, 2016, 179, 104-108.	1.3	36
100	Selective laser melting of AlSi10Mg: Influence of post-processing on the microstructural and tensile properties development. Materials and Design, 2016, 105, 212-222.	3.3	237
101	Adding functionality with additive manufacturing: Fabrication of titanium-based antibiotic eluting implants. Materials Science and Engineering C, 2016, 64, 407-415.	3.8	67
102	An iterative approach of hot isostatic pressing tooling design for net-shape IN718 superalloy parts. International Journal of Advanced Manufacturing Technology, 2016, 83, 1835-1845.	1.5	25
103	A new approach to develop palladium-modified Ti-based alloys for biomedical applications. Materials and Design, 2016, 109, 98-111.	3.3	26
104	Microstructure and strength of selectively laser melted AlSi10Mg. Acta Materialia, 2016, 117, 311-320.	3.8	380
105	Process optimisation of selective laser melting using energy density model for nickel based superalloys. Materials Science and Technology, 2016, 32, 657-661.	0.8	151
106	Selective laser melting of Invar 36: Microstructure and properties. Acta Materialia, 2016, 103, 382-395.	3.8	185
107	The development of TiNi-based negative Poisson's ratio structure using selective laser melting. Acta Materialia, 2016, 105, 75-83.	3.8	231
108	On the role of thermal fluid dynamics into the evolution of porosity during selective laser melting. Scripta Materialia, 2015, 105, 14-17.	2.6	172

#	Article	IF	CITATIONS
109	Optimisation of selective laser melting for a high temperature Ni-superalloy. Rapid Prototyping Journal, 2015, 21, 423-432.	1.6	68
110	In-situ shelling via selective laser melting: Modelling and microstructural characterisation. Materials and Design, 2015, 87, 845-853.	3.3	31
111	Influence of processing conditions on strut structure and compressive properties of cellular lattice structures fabricated by selective laser melting. Materials Science & Engineering A: Structural Materials: Properties, Microstructure and Processing, 2015, 628, 188-197.	2.6	289
112	Fabrication of large Ti–6Al–4V structures by direct laser deposition. Journal of Alloys and Compounds, 2015, 629, 351-361.	2.8	243
113	On the role of melt flow into the surface structure and porosity development during selective laser melting. Acta Materialia, 2015, 96, 72-79.	3.8	715
114	Microstructural control during direct laser deposition of a Î <sup>2</sup> -titanium alloy. Materials & Design, 2015, 81, 21-30.	5.1	70
115	Gel casting of sialon ceramics based on water soluble epoxy resin. Ceramics International, 2015, 41, 11534-11538.	2.3	12
116	Linear friction welding of Ti6Al4V: Experiments and modelling. Materials Science and Technology, 2015, 31, 372-384.	0.8	26
117	Validation of a Model of Linear Friction Welding of Ti6Al4V by Considering Welds of Different Sizes. Metallurgical and Materials Transactions B: Process Metallurgy and Materials Processing Science, 2015, 46, 2326-2331.	1.0	14
118	Selective laser melting of AlSi10Mg alloy: Process optimisation and mechanical properties development. Materials & Design, 2015, 65, 417-424.	5.1	866
119	The influence of the laser scan strategy on grain structure and cracking behaviour in SLM powder-bed fabricated nickel superalloy. Journal of Alloys and Compounds, 2014, 615, 338-347.	2.8	539
120	Rheological characterization and shape control in gel-casting of nano-sized zirconia powders. Ceramics International, 2014, 40, 14405-14412.	2.3	18
121	Effect of grain size reduction of AA2124 aluminum alloy powder compacted by spark plasma sintering. Journal of Alloys and Compounds, 2014, 609, 215-221.	2.8	42
122	Microstructural and texture development in direct laser fabricated IN718. Materials Characterization, 2014, 89, 102-111.	1.9	420
123	Stereological Analysis of the Microstructural Inhomogeneities in Direct-Chill Cast and Continuous-Cast Aluminium-Magnesium Alloy (AA5754). Praktische Metallographie/Practical Metallography, 2014, 51, 77-94.	0.1	0
124	Finite Element Modeling of the Inertia Friction Welding of Dissimilar High-Strength Steels. Metallurgical and Materials Transactions A: Physical Metallurgy and Materials Science, 2013, 44, 5054-5064.	1.1	20
125	Influence of the microstructural inhomogeneities on the martensite-to-austenite phase transformation temperatures in TiNiCu-based shape-memory alloys. Materials Chemistry and Physics, 2013, 141, 272-277.	2.0	3
126	Direct laser fabrication of three dimensional components using SC420 stainless steel. Materials & Design, 2013, 47, 731-736.	5.1	55

8

#	Article	IF	CITATIONS
127	Influence of hot isostatic pressing temperature on microstructure and tensile properties of a nickel-based superalloy powder. Materials Science & Engineering A: Structural Materials: Properties, Microstructure and Processing, 2013, 564, 176-185.	2.6	99
128	Microstructure and tensile properties of selectively laser-melted and of HIPed laser-melted Ti–6Al–4V. Materials Science & Engineering A: Structural Materials: Properties, Microstructure and Processing, 2013, 578, 230-239.	2.6	613
129	Friction welding of titanium alloys: addressing the structural integrity issues through process optimisation. , 2013, , 313-315.		1
130	Inertia friction welding (IFW) for aerospace applications. , 2012, , 25-74.		18
131	Deformation of microstructurally refined cast Ti46Al8Nb and Ti46Al8Ta. Intermetallics, 2012, 23, 1-11.	1.8	32
132	Microstructural and Residual Stress Development due to Inertia Friction Welding in Ti-6246. Metallurgical and Materials Transactions A: Physical Metallurgy and Materials Science, 2012, 43, 3149-3161.	1.1	20
133	Characterization of Dissimilar Linear Friction Welds of α-β Titanium Alloys. Journal of Materials Engineering and Performance, 2012, 21, 770-776.	1.2	28
134	In-Situ observation of primary $\hat{I}^3 \hat{a} \in 2$ melting in Ni-base superalloy using confocal laser scanning microscopy. Materials Characterization, 2011, 62, 760-767.	1.9	27
135	A synchrotron tomographic energy-dispersive diffraction imaging study of the aerospace alloy Ti 6246. Journal of Applied Crystallography, 2011, 44, 150-157.	1.9	12
136	Influence of the heating rate on the initiation of primary recrystallization in a deformed Al–Mg alloy. Scripta Materialia, 2010, 63, 371-374.	2.6	25
137	Comparative determination of the α/β phase fraction in α+β-titanium alloys using X-ray diffraction and electron microscopy. Materials Characterization, 2009, 60, 1248-1256.	1.9	43
138	Effect of the forging pressure on the microstructure and residual stress development in Ti–6Al–4V linear friction welds. Acta Materialia, 2009, 57, 5582-5592.	3.8	128
139	Influence of base metal microstructure on microstructural development in aluminium based alloy friction stir welds. Science and Technology of Welding and Joining, 2007, 12, 361-369.	1.5	34
140	Microstructure-microhardness relationships in friction stir welded AA5251. Journal of Materials Science, 2007, 42, 7299-7306.	1.7	27
141	Friction stir welding parameters: a tool for controlling abnormal grain growth during subsequent heat treatment. Materials Science & Engineering A: Structural Materials: Properties, Microstructure and Processing, 2005, 391, 51-59.	2.6	154
142	Influence of process parameters on superplasticity of friction stir processed nugget in high strength Al – Cu – Li alloy. Materials Science and Technology, 2004, 20, 1370-1376.	0.8	10
143	Influence of Forging Pressure on Microstructural and Mechanical Properties Development in Linear Friction Welded Al-Cu Dissimilar Joint. Soldagem E Inspecao, 0, 24, .	0.6	0
144	Making the most of additive layer manufacture - development of tailored titanium implants with embedded therapeutics. Frontiers in Bioengineering and Biotechnology, 0, 4, .	2.0	0